

# Establishment of a hepatocellular carcinoma patient-derived xenograft platform and its application in biomarker identification

Bo Hu<sup>1,2\*</sup>, Hong Li<sup>3\*</sup>, Wei Guo<sup>1,2,4</sup>, Yun-Fan Sun<sup>1,2</sup>, Xin Zhang<sup>1,2</sup>, Wei-Guo Tang<sup>1,2</sup>, Liu-Xiao Yang<sup>1,2</sup>, Yang Xu<sup>1,2</sup>, Xiao-Yan Tang<sup>3</sup>, Guo-Hui Ding<sup>3</sup>, Shuang-Jian Qiu<sup>1,2</sup>, Jian Zhou<sup>1,2,5</sup>, Yi-Xue Li<sup>3</sup>, Jia Fan<sup>1,2,5</sup> and Xin-Rong Yang<sup>1,2</sup> 

<sup>1</sup>Department of Liver Surgery, Liver Cancer Institute, Zhongshan Hospital, Fudan University, Shanghai, People's Republic of China

<sup>2</sup>Key Laboratory of Carcinogenesis and Cancer Invasion, Ministry of Education, Shanghai, People's Republic of China

<sup>3</sup>Key Laboratory of Computational Biology, CAS-MPG Partner Institute for Computational Biology, Shanghai Institutes for Biological Sciences, Chinese Academy of Sciences, Shanghai, People's Republic of China

<sup>4</sup>Department of Laboratory Medicine, Zhongshan Hospital, Fudan University, Shanghai, People's Republic of China

<sup>5</sup>Institute of Biomedical Sciences, Fudan University, Shanghai, People's Republic of China

Using a method optimized in hepatocellular carcinoma (HCC), we established patient-derived xenograft (PDX) models with an increased take rate (42.2%) and demonstrated that FBS +10% dimethyl sulfoxide exhibited the highest tumor take rate efficacy. Among 254 HCC patients, 103 stably transplantable xenograft lines that could be serially passaged, cryopreserved and revived were established. These lines maintained the diversity of HCC and the essential features of the original specimens at the histological, transcriptome, proteomic and genomic levels. Tumor engraftment was associated with lack of encapsulation, poor tumor differentiation, large size and overexpression of cancer stem cell biomarkers, and was an independent predictor for overall survival and tumor recurrence after resection. To confirm the preclinical value of the PDX model in HCC treatment, several antitumor agents were tested in 16 selected PDX models. The results revealed a high degree of pharmacologic heterogeneity in the cohort, as well as heterogeneity to different agents in the same individual. The sorafenib responses observed between HCC patients and the corresponding PDXs were also consistent. After molecular characterization of the PDX models, we explored the predictive markers for sorafenib response and found that mitogen-activated protein kinase kinase kinase 1 (MAP3K1) might play an important role in sorafenib resistance and sorafenib response is impaired in patients with MAP3K1 downexpression. Our results indicated that PDX models could accurately reproduce patient tumors biology and could aid in the discovery of new treatments to advance in precision medicine.

\*B.H. and H.L. contributed equally to this work

**Additional Supporting Information** may be found in the online version of this article.

**Key words:** hepatocellular carcinoma, patient-derived tumor grafts, sorafenib, drug resistance, MAP3K1

**Abbreviations:** AFP: serum a-fetoprotein; CSC: cancer stem cell; HCC: hepatocellular carcinoma; MAP3K1: mitogen-activated protein kinase kinase kinase 1; mRECIST: modified response evaluation criteria in solid tumors; OS: overall survival; PDX: patient-derived xenograft; TTR: time to recurrence.

**Conflicts of interest:** None declared.

**Grant sponsor:** National High Technology Research and Development Program (863 Program) of China; **Grant number:** 2015AA020401;

**Grant sponsor:** National Key Sci-Tech Project; **Grant numbers:** 2013ZX10002010-003, 2013ZX10002010-004, 2013ZX10002011-004,

2012ZX0930100-007; **Grant sponsor:** National Natural Science Foundation of China; **Grant numbers:** 81802364, 81772551, 81672839,

81472676, 81572064, 81572823, 81502028, 81572884, 81372317; **Grant sponsor:** Projects from the Shanghai Science and Technology

Commission; **Grant numbers:** 13140901900, 14DZ1940300, 14411970200, 14140902301; **Grant sponsor:** State Key Program of National

Natural Science of China; **Grant number:** 81530077; **Grant sponsor:** Chinese Academy of Sciences; **Grant numbers:** 12020105, 12020103,

XDA12010201; **Grant sponsor:** Shanghai Municipal Commission of Science and Technology; **Grant number:** 15YF1414100; **Grant sponsor:**

Specialized Research Fund for the Doctoral Program of Higher Education and Research Grants Council Earmarked Research Grants Joint

Research Scheme; **Grant number:** 20130071140008

**DOI:** 10.1002/ijc.32564

**History:** Received 9 Aug 2018; Accepted 11 Jun 2019; Online 16 Jul 2019

**Correspondence to:** Xin-Rong Yang, MD, PhD, Liver Cancer Institute, Fudan University, 136 Yi Xue Yuan Road, Shanghai 200032, People's Republic of China, Tel.: & Fax: +86-21-64037181, Fax: +86-21-64037181, E-mail: yang.xinrong@zs-hospital.sh.cn

**What's new?**

Patient-derived xenografts (PDX) models offer a promising preclinical tool. Here, the authors established the largest bank of hepatocellular carcinoma (HCC) PDX models with a high and stable tumor take rate that recapitulated the key clinical and molecular characteristics of primary tumors. The tumor take rate was associated with expression of cancer stem cell proteins, lack of tumor encapsulation, poor differentiation, advanced stage, overall survival, and time to recurrence in patients. The models were used to identify MAP3K1 expression as an indicator of patient response to sorafenib treatment. PDX models are valuable surrogates for HCC patients and could facilitate translational research.

**Introduction**

Hepatocellular carcinoma (HCC) is the second leading cause of cancer-related deaths worldwide, with continually increasing incidence rates.<sup>1,2</sup> Surgery remains the most effective curative treatment, though only 30–40% of HCC patients are suitable for surgical intervention.<sup>3</sup> The lack of effective medical treatment results in dismal outcomes for the remaining patients.<sup>4</sup> Although the multikinase inhibitor sorafenib was recently approved as a standard treatment for patients with advanced HCC, the survival benefits remain unclear<sup>5,6</sup> due to a lack of suitable preclinical models that recapitulate the pathologic, biological and genetic features of HCC.<sup>7</sup>

Patient-derived xenograft (PDX) models, which directly graft fresh tumor tissues into immunosuppressed mice, have been regarded as valuable preclinical models for oncology drug development and drug response prediction.<sup>8</sup> Without prior selection in tissue culture, PDX models can recapitulate human tumor biology more accurately than traditional cell line-derived xenografts.<sup>7,9,10</sup> HCC is an extremely heterogeneous disease with complex molecular and genetic pathogenesis; the PDX models provide an ideal preclinical model for assessing novel therapies and understanding molecular and cellular mechanisms that contribute to tumorigenesis.<sup>11,12</sup> Despite a recent study reporting the clinical relevance of PDX models in HCC (~26% tumor take rate),<sup>13</sup> additional studies focusing on methods for establishing and preserving resemblance to the original tumor and on the predictive value of the PDX models in the preclinical evaluation of treatment modalities are required before its widespread use in the HCC preclinical setting.

Here, we optimized a technique for PDX model engraftment and preservation with a high and stable tumor take rate. A large panel of PDX models was established that retain the histological characteristics and genetic heterogeneity of the original tumor ( $F_0$ ) even after serial passage ( $F_6$ ) or cryopreservation. Furthermore, we found that the tumor take rate was significantly associated with expression of cancer stem cell (CSC) proteins, lack of tumor encapsulation, poor differentiation, advanced BCLC stage, tumor size and number, overall survival (OS) and time to recurrence (TTR) in patients. Based on transcriptomic and genomic data, we also conducted a proof-of-concept study to identify new molecular biomarkers for resistance to sorafenib in PDX models that were clinically validated in HCC patients. Mitogen-activated protein kinase kinase kinase 1 (MAP3K1) may play an

important role in sorafenib resistance in PDX models. This PDX model showed great promise in a preclinical setting for biomarker development, understanding the mechanisms of drug resistance, drug screening and personalized medicine applications for HCC patients.

**Materials and Methods****Patients and tumor samples**

This study was approved by the Institutional Review Board of Zhongshan Hospital and complied with the standards of the Declaration of Helsinki and current ethical guidelines. After patients provided written informed consent, HCC samples were obtained from October 2012 to March 2016. Tumor samples were transferred in ice-chilled high-glucose Dulbecco's modified Eagle medium (DMEM; Gibco, 11965092) supplemented with 100 U/ml penicillin and 100 U/ml streptomycin for engraftment within 2 hr after resection. Samples were snap-frozen in liquid nitrogen for molecular characterization and fixed in alcohol-formalin-acetic acid solution or paraffin-embedded for histopathological analysis. Similar sample processing was conducted on tumors collected from mice. The overall flow chart of PDX program was shown in Figure 1.

**Follow-up and treatment for tumor recurrences**

Patients were followed up every 2 months during the first postoperative year and at least every 3–4 months afterward. All patients were monitored prospectively by serum  $\alpha$ -fetoprotein (AFP), abdomen ultrasonography and chest X-ray every 1–6 months, according to the postoperative time. For patients with test results suggestive of recurrence, computed tomography and/or magnetic resonance imaging were used to verify whether intrahepatic recurrence and/or distal metastasis had occurred. A diagnosis of recurrence was based on typical imaging appearance in computed tomography and/or magnetic resonance imaging scan and an elevated AFP level. Patients with confirmed recurrence received further treatment, which followed the same protocol based on tumor size, site, number of tumor nodules and liver function. Briefly, if the recurrent tumor was localized, a second liver resection, radiofrequency ablation or percutaneous ethanol injection was suggested. If the recurrent tumor was multiple or diffused, transcatheter arterial chemoembolization was the choice. External radiotherapy was given if lymph node or bone metastasis was found. Otherwise, symptomatic treatment was provided.

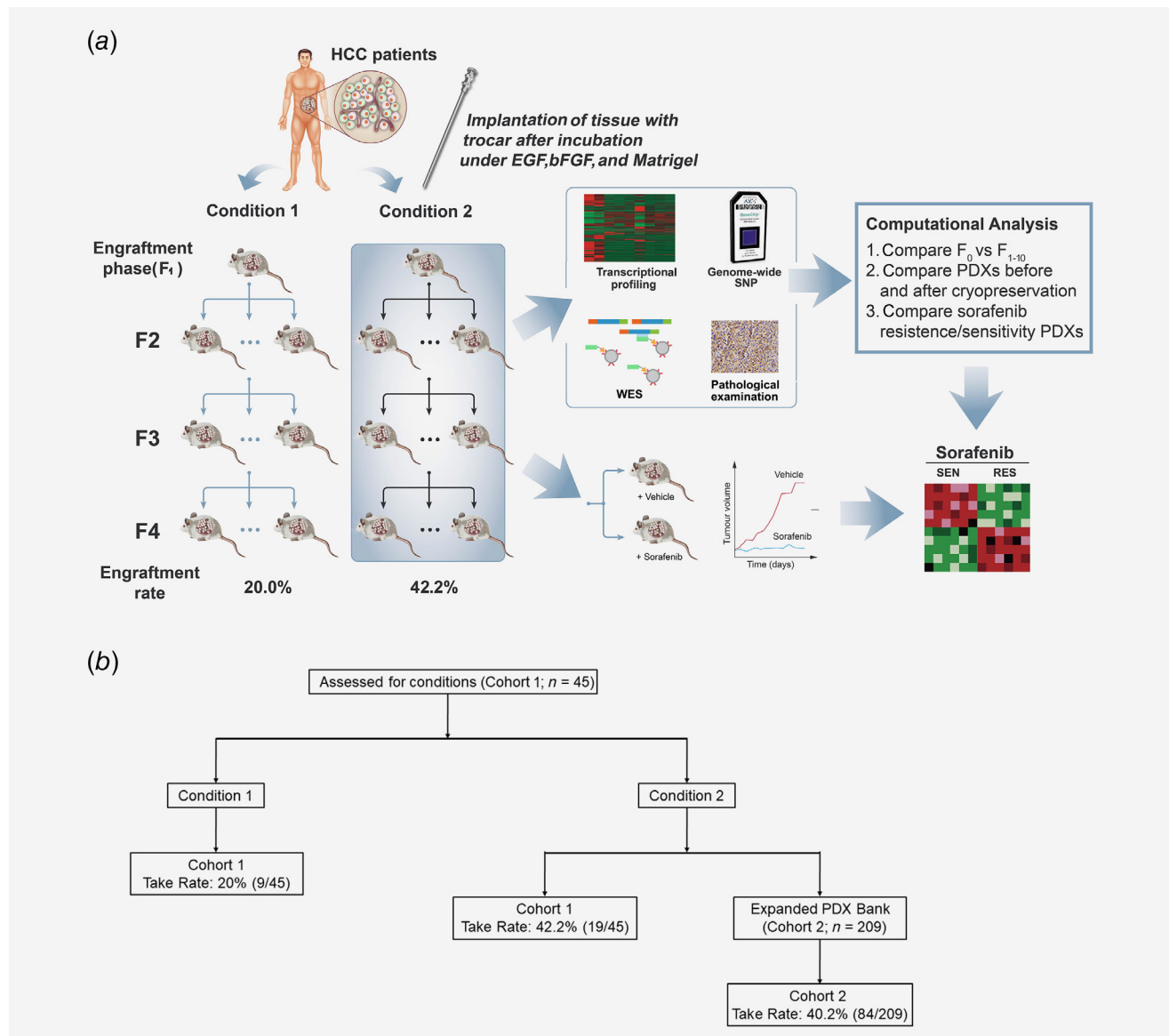


**Figure 1.** Flowchart of the PDX program. (a) The overall flow chart of PDX program. (b) Experimental design of selecting an optimized method. Abbreviations: RES, resistant; SEN, sensitive.

### The cell line

The human HCC cell line MHCC97H (RRID: CVCL\_4972; Liver Cancer Institute, Fudan University, China) have been authenticated using STR profiling within the last 3 years and was maintained in DMEM containing high glucose (Gibco BRL, Grand Island, NY), 10% heat-inactivated fetal bovine serum (Gibco BRL) at 37°C in a humidified atmosphere containing 5% CO<sub>2</sub>.

### Establishment of xenografts

Fresh tumor tissues were placed in ice-chilled high-glucose DMEM with 10% FBS, 100 U/ml penicillin and 100 U/ml streptomycin and rapidly processed for engraftment. After removal of necrotic tissue, tumor specimens were partitioned into

2 × 1 × 1 mm<sup>3</sup> sections with a No.10 scalpel blade under aseptic conditions and washed three times in ice-cold PBS. Tissue fragments were incubated in DMEM with 10% FBS, 100 U/ml penicillin and 100 U/ml streptomycin (Condition 1) or in DMEM medium supplemented with 50% Matrigel™ (BD, Franklin Lakes, NJ; 356234), 10 ng/ml epidermal growth factor (Gibco, Waltham, MA; PHG0314), 10 ng/ml basic fibroblast growth factor (Gibco; PHG0264), 100 U/ml penicillin and 100 U/ml streptomycin (Condition 2) for 30 min. Sections from each sample were processed under both conditions to compare efficiency. Three pieces of tumor tissues with the incubation mix (Matrigel plus growth factors) were transplanted into the right flanks of male nonobese, diabetic, severe combined immunodeficiency (NOD/SCID) mice (*n* = 3;

4–5 weeks old, Shanghai Institute of Material Medicine, Chinese Academy of Science) subcutaneously with a No. 20 trocar. Animal care and experimental protocols were approved by the Shanghai Medical Experimental Animal Care Commission. Tumor growth was recorded three times per week by measuring the length (L) and width (W) with a caliper. Tumor volume (TV, mm<sup>3</sup>) was calculated as  $TV = 0.5 \times L \times W^2$ . Mice were sacrificed at approximately 30 days or up to 80 days after grafting. Grafts were collected for histological evaluation, re-grafting or snap-freezing in liquid nitrogen.

### Tumor specimen cryopreservation

Ten xenograft tumors were selected and each tumor was divided into 18 fragments, which were then equally distributed into six groups using different cryoprotectant agents. The composition of these six experimental groups were: DMEM+10% dimethyl sulfoxide (DMSO; DD), FBS + 10% DMSO (FD), DMEM+10% glycerol (DG), FBS + 10% glycerol (FG), DMEM+5% DMSO+5% glycerol (DDG) and FBS + 5% DMSO+5% glycerol (FDG). Sliced tumor tissues in sterile cryotubes (Greiner-Bio-One, Frickenhausen, Germany) within a freezing container (Nalgene, Rochester, NY, C1562) were placed immediately at  $-80^{\circ}\text{C}$  overnight and then transferred to liquid nitrogen. Thawing tests were conducted 6 months after freezing. Liquid nitrogen cryopreserved tumor pieces were thawed in a  $37^{\circ}\text{C}$  water bath and processed in the same manner as for xenograft establishment. Mice were sacrificed when tumors were greater than 1,500 mm<sup>3</sup> or up to 3 months after transplantation.

### Histology and the molecular features analysis

For histopathology, routine hematoxylin–eosin (H&E) staining was performed. The diagnosis of HCC was confirmed by two independent pathologists. To investigate the similarity between xenografts and the original patient tumors, the gene expression profiles, SNP genotypes, somatic mutations and protein expression of marker genes were compared as previously described<sup>14,15</sup> and the detailed methodologies were described in Supporting Information Materials and Methods. Antibodies and evaluation of immunohistochemical variables are addressed in Supporting Information Table S1.

### In vivo pharmacologic studies

**Drugs.** Sorafenib, 5-Fluorouracil (5-FU), oxaliplatin and doxorubicin were purchased from Sigma. Controls were treated with dimethyl sulfoxide (DMSO) concentrations equal to the highest combination groups (maximum 0.3% DMSO).

**Chemotherapy.** When TV reached 100–150 mm<sup>3</sup>, animals were randomly distributed into sorafenib, 5-FU, oxaliplatin and doxorubicin groups ( $n = 4-6$  per group). Mice received sorafenib (30 mg/kg orally, once per day), 5-FU (10 mg/kg, intraperitoneally, five times per week), oxaliplatin (12.5 mg/kg, intravenous injection, once per week), doxorubicin (1 mg/kg, intravenous injection, once every 3 days) or vehicle control

for 30 days. Bodyweight, ascites formation and OS were monitored daily.

**Tumor growth inhibition.** Changes in TV were calculated for each mouse by subtracting the TV on a specified observation day from the TV at the start of therapy as follows: Tumor growth inhibition (TGI;  $\Delta T/\Delta C$  value) =  $\Delta T/\Delta C$  (%), where  $T$  = Treated TVs and  $C$  = control TVs. According to the criteria of the Division of Cancer Treatment (NCI), we defined a response as 0–20% TGI, stability as 21–50% TGI and tumor progression as >50% TGI.<sup>16</sup>

### Statistical analysis

Statistical analyses were performed using IBM SPSS 20.0 software (SPSS, Chicago, IL). Additional details are provided in the Supporting Information Materials and Methods.

### Data availability

The complete dataset is available as GEO proles on the GEO (Gene Expression Omnibus) database ([www.ncbi.nih.gov/geo/](http://www.ncbi.nih.gov/geo/); GEO Accession No. GSE90653).

## Results

### Establishment of the PDX model with high and stable tumor take rates

To compare the difference of tumor take rate between Condition 1 and Condition 2, tumor tissues from 45 HCC patients were implanted in NOD/SCID mice under both conditions (Fig. 1a). Ten transplantable PDX models (22.2%; 10/45) were established under Condition 1, but only nine were ultimately established (20.0% stable take rate). Twenty transplantable PDX models (44.4%; 20/45) were established under Condition 2, and 19 were successfully maintained through multiple rounds of serial transplantation (42.2% stable take rate), which was higher than in recent studies.<sup>10,17,18</sup> After we confirmed Condition 2 was better in xenograft, we then used Condition 2 to construct the PDX models in further study ( $n = 209$ ), and 84 cases were succeeded (84/209, 40.19%). Thus, total of 254 cases were used to construct PDX models with Condition 2, 103 xenograft lines were finally constructed and the total take rate was 40.6% (103/254; Fig. 1b). The clinical characteristics of 254 HCC patients were shown in Table 1.

In the hierarchical clustering of expression profiles (Fig. 2a), tumor samples from the same patient (the original tumor or tumors of PDXs) were clustered together, and all tumor-surrounding samples were clustered together. In the hierarchical clustering of SNP genotypes (Fig. 2b), samples from the same patient were clustered together, indicating the similar genome origin. Moreover, PDXs and their original patient tumor harbored highly similar somatic mutation patterns (Supporting Information Fig. S1A). For genes that are frequently mutated in HCC patients, mutations of PDXs were exactly the same with mutations in the original tumor (Supporting Information Fig. S1B).

Table 1. Patient, primary tumor and xenograft characteristics

Clinical and pathological		No. of patients	Establishment of xenografts		<i>p</i>
Indexes		<i>n</i> = 254	No	Yes	
Age (years)	≤50	118	69	49	0.768
	>50	136	82	54	
Sex	Female	40	25	15	0.669
	Male	214	126	88	
Liver cirrhosis	No	55	33	22	0.710
	Yes	199	118	81	
HBsAg	Negative	40	16	24	0.696
	Positive	214	135	79	
ALT (U/l)	≤75	146	83	63	0.113
	>75	108	68	40	
AFP (ng/ml)	≤20	115	70	45	0.675
	>20	139	81	58	
Tumor encapsulation	Complete	131	88	43	<b>0.010</b>
	None	123	63	60	
Tumor differentiation	I–II	145	101	44	<b>0.000</b>
	III–IV	109	50	59	
Tumor size (cm)	≤5	124	108	16	<b>0.000</b>
	>5	130	43	87	
Tumor number	Single	212	144	68	<b>0.001</b>
	Multiple	42	7	35	
Vascular invasion	No	169	104	65	0.339
	Yes	85	47	38	
BCLC	0 + A	154	102	52	<b>0.006</b>
	B + C	100	49	51	

Bold values indicated  $p < 0.05$ .

Abbreviations: AFP, alpha-fetoprotein; ALT, alanine aminotransferase; BCLC, the Barcelona Clinic Liver Cancer staging; HBsAg, hepatitis B surface antigen.

These results demonstrate that PDXs represent the transcriptomic and genomic characteristics of the original patient tumors.

In addition, we found the tumor growth rates for the different passages tended to increase during serial transplantation, but there had no significant differences ( $p = 0.085$ , Supporting Information Fig. S2).

#### Cryopreservation of xenograft tumor tissues in various cryoprotectants

Ten F<sub>2</sub> xenograft tumor tissue lines were frozen in six different cryoprotectants and preserved in liquid nitrogen for 6 months. To evaluate the tumorigenicity of the cryopreserved tissues, we subcutaneously transplanted these tissues into the right flank of NOD/SCID mice (three mice per tumor sample, 10 mice per agent). The tumor take rates of the cryopreserved xenograft tissues were 100, 60, 40, 40, 40 and 50% in the FD, DGD, DD, DG, FG and FGD groups, respectively. The take rate in the FD group was higher than the corresponding take rates in the DD, DG, FG and FGD groups ( $p < 0.05$ ), but there was no statistically significant difference between the FD

and DGD groups ( $p = 0.087$ ; Supporting Information Table S2). Ultimately, FD was selected for cryopreservation of the xenograft tumors. A biobank was established for all models and the thawing success rate reached 92.3%, which was close to our tumor take rate on fresh samples (97.2% at F<sub>2</sub>–F<sub>6</sub>). The cryopreserved xenografts exhibited volume-doubling times greater than 2 months and they closely recapitulated the histology of fresh xenografts (Fig. 2c). Cluster analysis of the gene expression and SNP genotype data also showed that PDX models generated from fresh or cryopreserved tissues clustered together and their mean similarities were 0.96 and 0.97, respectively (Figs. 2d and 2e).

#### Recapitulation of the morphological, pathological and molecular features of patient tumors in tumor xenografts

Histological analysis of our panel demonstrated a concordance between xenografts (between F<sub>1</sub> and F<sub>6</sub>) and the corresponding patient tumors in terms of tumor differentiation. Using histological grading of HCC, xenografts were classified as well-differentiated (4/103, 3.9%), moderately differentiated (47/103, 45.6%) or poorly differentiated (52/103, 54.7%; Fig. 3a).

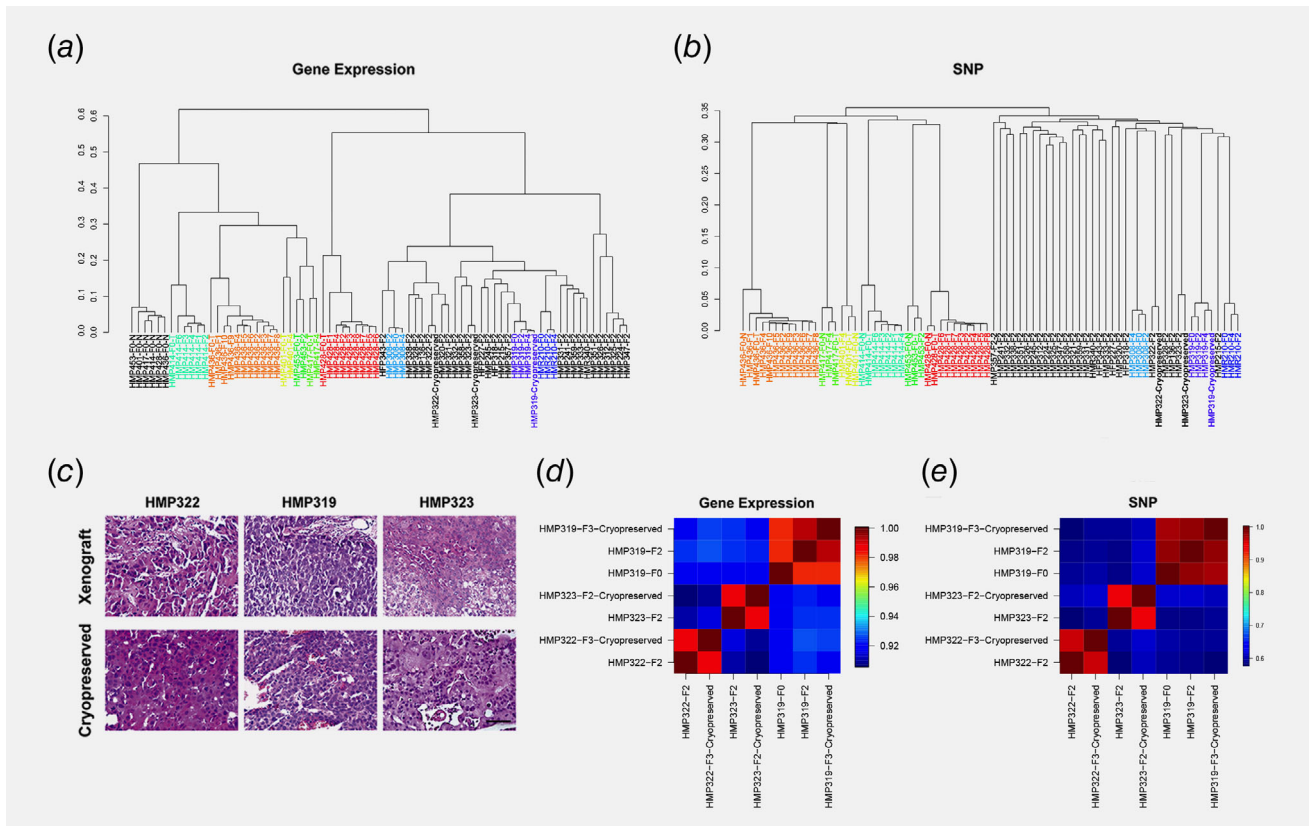


**Figure 2.** Clustering of PDXs at the genomic level. (a) and (b) Xenograft lines were evaluated by hierarchical clustering using gene expression and SNP genotype data. (c) Sections from F<sub>2</sub> xenografts before cryopreservation (up) are shown, and the corresponding xenograft after cryopreservation (down) shows conserved morphology (H&E); magnification 400 $\times$ . (d) and (e) Xenograft lines before or after cryopreservation are clustered together with respect to gene expression and SNPs. Xenograft ID (HM(F)P-###), transplant generation number (F<sub>#</sub>) and cryopreservation are shown for each branch of the dendrogram. Three xenograft lines obtained from the same patient are designated by color. The highest (red) and lowest (blue) correlation was used to cluster the xenografts by their overall correlation. Abbreviations: N, nontumor; T, tumor.

HCC associated proteins, such as alpha-fetoprotein (AFP), proliferation protein for Ki67, apoptosis protein for caspase-3 and intermediate filament protein for vimentin, were immunohistochemically evaluated in tumor tissues. Original tumors were compared to F<sub>1</sub>–F<sub>6</sub> serially transplanted xenografts; all tumor grafts retained the major characteristics of their matched primary tumor over multiple passages (Fig. 3b). Human vimentin was absent ( $p < 0.05$ ). Genes downregulated in the mouse xenografts were significantly enriched in the extracellular matrix ( $p < 0.001$ ), the major component of tumor stroma. Thus, a percentage of the human stroma was gradually lost during serial engraftment.

Due to its clinical utility, AFP secretion in the blood of PDXs was evaluated. A pilot study with sera from all the xenografts and the corresponding patients was conducted, revealing that 56.3% (58/103) of HCC patients were AFP positive (>20 ng/ml) compared to 55.3% (57/103) in xenografts. Additionally, the AFP levels in 80.1% (83/103) of the xenografts (median, 376.3; range, 0 to >60,500) were consistent with corresponding levels in patients (median, 272.4; range, 2 to >60,500;  $r = 0.626$ ,  $p < 0.001$ ; Fig. 3c).

Genome-wide similarities between patient tumors (F<sub>0</sub>) and mouse xenografts (F<sub>1</sub>–F<sub>10</sub>) were evaluated. Gene expression

data from PDX models obtained from the same patient clustered together with a mean similarity of 0.92 (Fig. 3d), which was significantly higher than in randomly selected samples. Therefore, PDX presented gene expression features of the original tumors and demonstrated robust similarities during distant transplantation. The mean similarity of SNP genotypes was 0.97 between patient tumors and xenografts (Fig. 3e). The xenografts recapitulated the profile of original tumors histologically, biologically and genetically.

### Prognostic value of tumor xenografts

The results of Kaplan–Meier analyses indicated that stable growth of the tumor engraftments was associated with shorter OS (median, 29.75 months *versus* not researched;  $p < 0.0001$ ; Fig. 4a) and TTR (median, 14.25 months *vs.* not researched;  $p < 0.0001$ ; Fig. 4a).

Univariate analyses indicated the ability to engraft was a prognostic factor for OS (Supporting Information Table S3) and TTR (Supporting Information Table S4) and the ability to stably engraft was an independent prognostic factor for OS (hazard ratio, 2.314; 95% confidence interval, 1.51–3.01;  $p = 0.017$ ) and TTR (hazard ratio, 1.752; 95% confidence

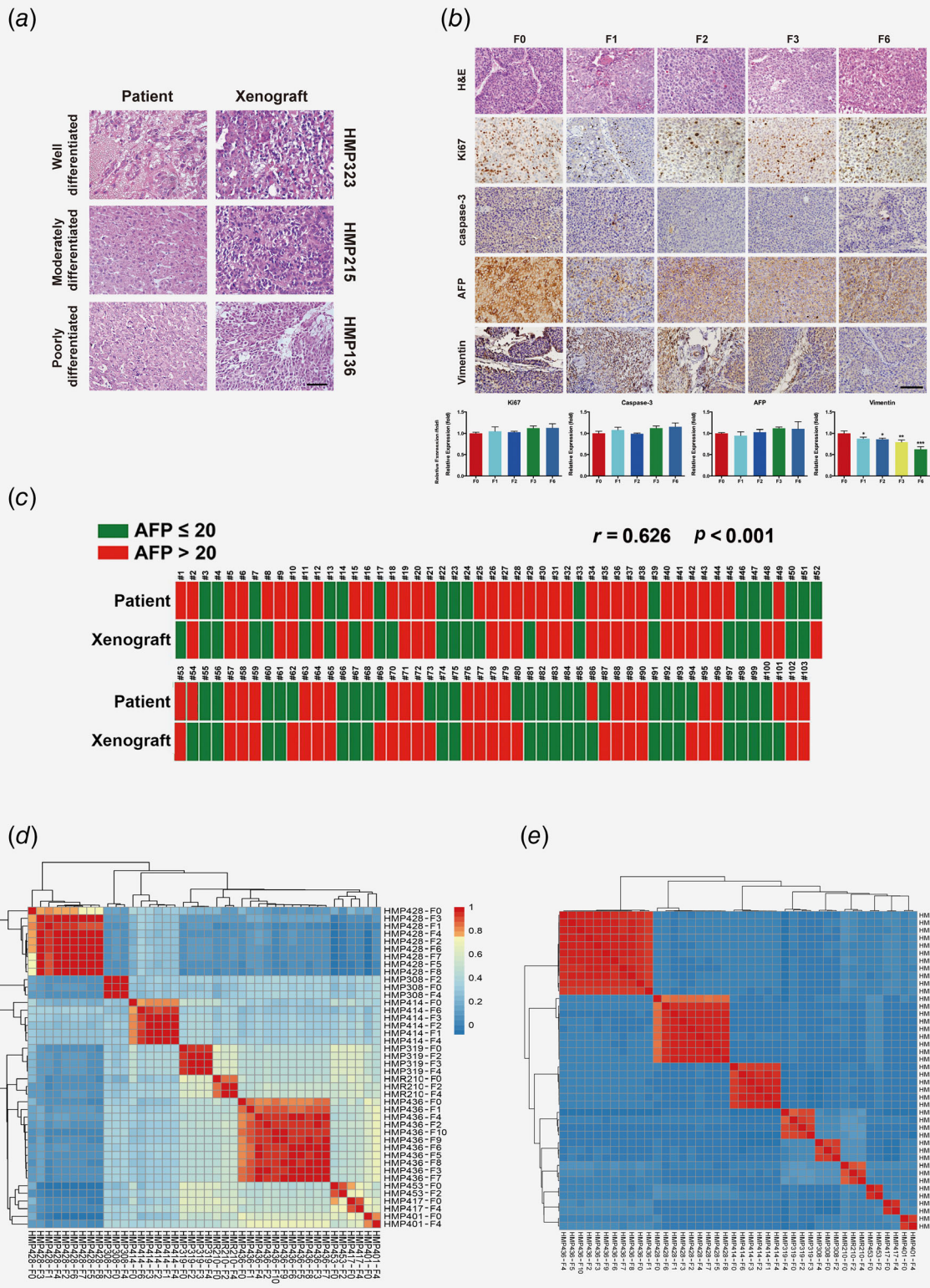


**Figure 3.** PDX models recapitulated the patient tumors from which they were derived. (a) Representative hematoxylin and eosin staining of patient tumors and corresponding F<sub>2</sub> xenografts for poorly differentiated (HMP323), moderately differentiated (HMP215) and well-differentiated (HMP136) cases; magnification 400x. (b) One representative patient sample (HMP319) showing retained pathology and antibody (Ki67, caspase-3, AFP and vimentin) status as xenografts over several passages (F<sub>1</sub>–F<sub>6</sub>); magnification 200x. \**p* < 0.05, \*\**p* < 0.01, \*\*\**p* < 0.001. (c) Comparison of AFP in models with serum from the corresponding patient. (d) and (e) Xenograft lines clustered together over sequential passages with respect to gene expression and SNPs.

interval, 1.28–2.41;  $p = 0.028$ ) based on multivariate analyses.

**Association of the xenograft take rate with clinical characteristics and CSC biomarkers**

Fisher’s exact tests were used to identify clinical parameters that were associated with high tumor take rates (Table 1). A high probability of *in vivo* tumor take rates

was significantly correlated with poor tumor differentiation ( $p = 0.001$ ). We compared the expression of CSC biomarkers, including EpCAM, CD133, CD13 and CD90 in 28 selected pairs of stable/no growth HCC samples. Over-expression of these proteins, which are involved in the successful generation of xenografts, was observed in stable growth samples ( $p < 0.05$ , Supporting Information Table S5 and Fig. 4b).

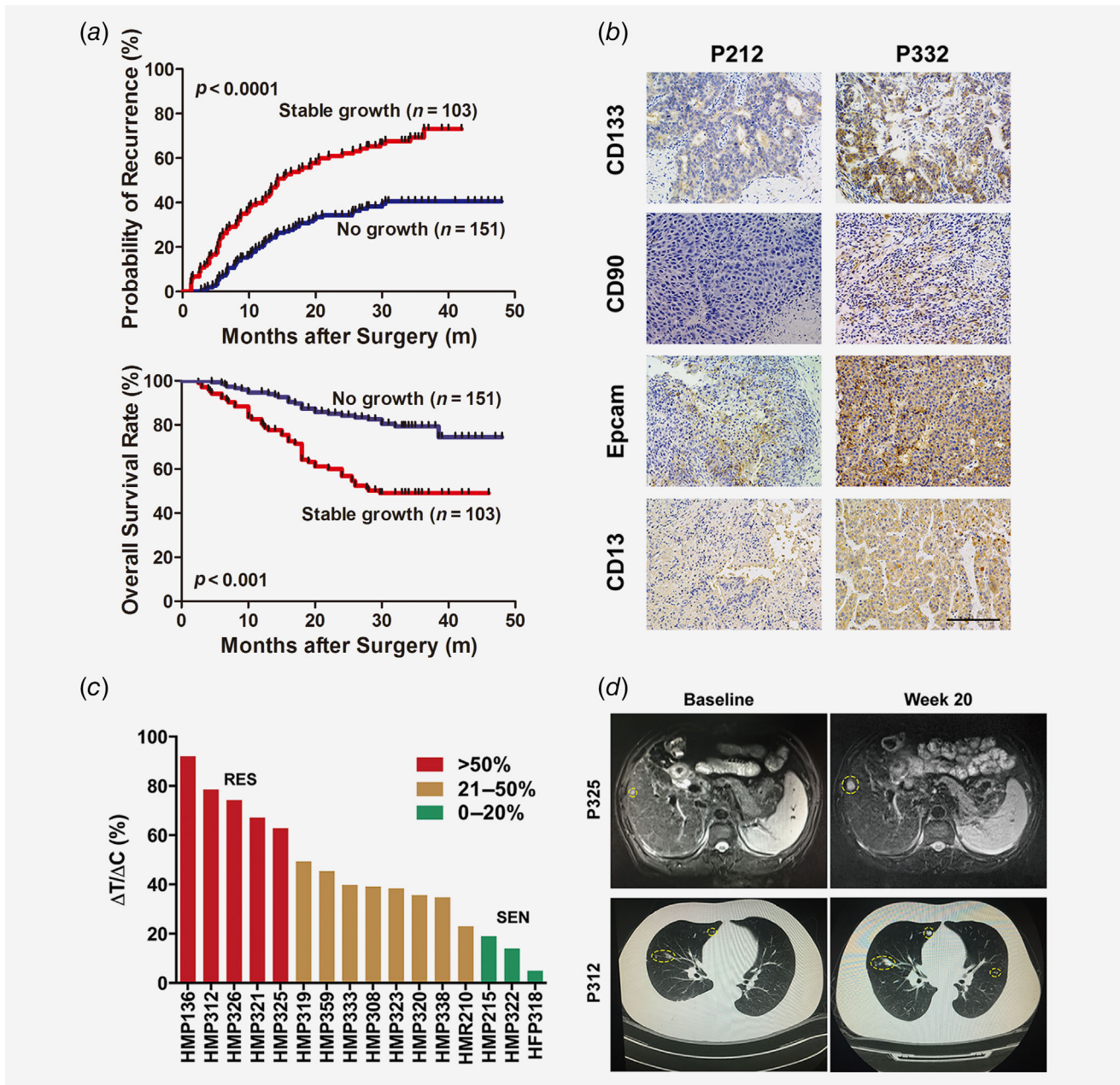


**Figure 4.** Association of the xenograft take rate with clinical characteristics and CSC biomarkers. (a) The Kaplan–Meier analysis of OS and time to recurrence for the stable growth of engrafts. (b) Representative CD133, CD90, EpCAM and CD13 immunostaining images; magnification 200x. (c) Waterfall plot of sorafenib response after 4 weeks of treatment in 16 cases. Sensitive, stable and resistant cases are shaded in light green, yellow and red, respectively. Abbreviations: RES, resistant; SEN, sensitive. (d) Computed tomography scans of two PDX models corresponding to advanced HCC patients receiving sorafenib treatment.

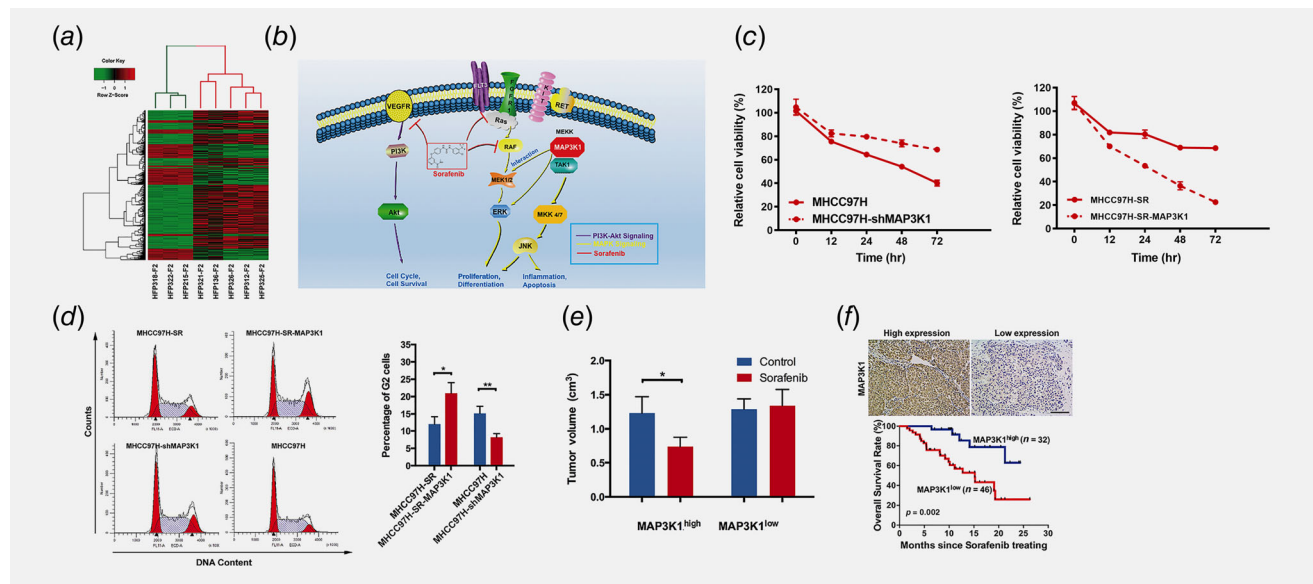


**Figure 5.** Practical value of PDX models in biomarker discovery of sorafenib. (a) Heat map indicating differentially expressed transcripts between the sensitive and resistant xenografts. Each colored square represents the relative transcript abundance for each sample, with the highest expression being red, average expression being black, and the lowest expression being green. (b) Schematic depiction of the role of MAP3K1 involving in sorafenib resistance. (c) Cell proliferation in HCC cell lines as indicated was assessed by CCK8 assays. (d) Cell cycle in HCC cell lines as indicated was detected by FCM. (e) Comparison of tumor volume between the PDX models with high and low *MAP3K1* expression treated with sorafenib. (f) Differences in *MAP3K1* expression between the sensitive and resistant cases and the comparison of OS between patients with high and low *MAP3K1* expression treated with sorafenib; magnification 400 $\times$ . \* $p < 0.05$ , \*\* $p < 0.01$ , \*\*\* $p < 0.001$ .

### Application of PDX models in predicting patient response to anticancer drugs

To explore the application of PDX models for predicting patient responses to targeted agents and chemotherapeutics, PDX models were treated with sorafenib or cytotoxic agents (5-FU, oxaliplatin or doxorubicin). Antitumor responses varied widely across the PDX models (Supporting Information Fig. S3). The TGIs of sorafenib and cytotoxic agents were remarkably different in the HMP391, HMP209 and HMP397 models.

To identify the intrinsic chemosensitivity of each tumor model to sorafenib, 16 tumor models were selected from 30 xenograft lines which were subjected to SNP genotyping and gene expression analysis. Approximately 30 days after dosing was initiated, the  $\Delta T/\Delta C$  values varied from 92.0% to 4.8% (Fig. 4c). Sorafenib induced tumor stabilization in three (HMP322, HMP215 and HFP318) of the 16 PDX models ( $\Delta T/\Delta C < 20\%$ ), whereas five models (HMP321, HMP312, HMP326, HMP325 and HMP136) were resistant to this agent ( $\Delta T/\Delta C > 50\%$ ). According to clinical data, two (HMP312 and HMP325) of the 16 corresponding xenograft patients (P312 and P325) received sorafenib treatment (>4 months) after tumor recurrence. Both patients exhibited progressive disease according to modified Response Evaluation Criteria in Solid Tumors (mRECIST), which was similar to the treatment response observed in the corresponding models (Fig. 4d). Patient P312 died from lung metastases within 10 months.

### Application of PDX models for the identification of predictive markers for sorafenib responses

We compared the SNP genotypes and gene expression profiles between three sorafenib-sensitive and five sorafenib-resistant PDX models and found 336 SNVs whose genotypes were completely different between the two groups. However, their  $p$ -values did not reach the genome-wide significance ( $p = 1e-8$ ) due to the small sample size. Almost all of them were located in nonexonic regions and have unclear functions. For gene expression, we uncovered 690 differentially expressed genes (Fig. 5a; Supporting Information Table S6). Functional analyses showed that differential genes were enriched in multiple signaling transduction pathways and molecular mechanisms of cancer (Supporting Information Fig. S4 and Table S7). As a multikinase inhibitor, sorafenib targets both Ras/Raf/MEK/ERK and PI3K-AKT pathways. The Ras/Raf/MEK/ERK pathway is the classical MAP kinase pathway. Additionally, Jun amino-terminal kinases (JNK) signaling pathway is the second most widely studied MAPK cascade. Seven genes (MINK1, SHC1, MAP3K12, CDC42, MAP3K1, ZAK and MAP3K2) in the JNK signaling pathway were differentially expressed, suggesting correlation with sorafenib response. MAP3K1 is an important component of the JNK cascade and also scaffolds the Ras/Raf/MEK/ERK cascade by binding to Raf-1, MEK1 and ERK2 (Fig. 5b).<sup>19</sup> Therefore, we focused our investigations on MAP3K1.

We validated the association between MAP3K1 and sorafenib sensitivity in cell lines, PDX models and patient tissues. We developed sorafenib-resistant HCC cells by continuous administration

of gradually increasing sorafenib concentrations over 6 months *in vitro*. Sorafenib resistance was accomplished in MHCC97H (MHCC97H-SR) cell. shRNA-mediated knockdown of MAP3K1 in MHCC97H cells and overexpression of MAP3K1 expression in MHCC97H-SR cell were confirmed using mRNA and protein analyses (Supporting Information Fig. S5). *In vitro* CCK8 assays showed that cell proliferation was significantly increased in MHCC97H cell after MAP3K1 inhibition under sorafenib treatment (10  $\mu$ M), and decreased in the MHCC97H-SR cell under the same treatment (Fig. 5c). Overexpression of MAP3K1 in MHCC97H-SR cell resulted in fewer cells in G2/M phase after sorafenib treatment for 48 hr. However, MAP3K1 inhibition in MHCC97H cell resulted in an increased proportion of cells in G2/M phase after sorafenib treatment for 48 hr (Fig. 5d). We examined the sorafenib therapy in MAP3K1 overexpression (HMP209, HFP227 and HMP241) and low expression (HMP328, HMP331 and HMP332) PDX models. Compared to the MAP3K1<sup>low</sup> cohorts, TVs were significantly inhibited by sorafenib in the MAP3K1<sup>high</sup> cohort (mean 0.736 vs. 1.338;  $p = 0.037$ ; Fig. 5e).

We examined the predicted role of MAP3K1 in 78 HCC patients with postsurgical tumor recurrence receiving sorafenib treatment. Patients were divided into low/high groups according to immunostaining results. All baseline patient parameters are described in Supporting Information Table S8. Compared to the MAP3K1<sup>high</sup> group, the MAP3K1<sup>low</sup> group exhibited shorter survival times (median, 15.20 months vs. not reached;  $p = 0.006$ ; Fig. 5f). Univariate and multivariate analyses demonstrated that the SII correlated was significantly prognostic OS (HR, 0.122; 95% CI, 0.04–0.38;  $p < 0.001$ ; Supporting Information Table S9). Thus, MAP3K1 expression may serve as a valuable indicator for selecting patients who are suitable for sorafenib treatment.

## Discussion

Due to the inability to accurately recapitulate the key aspects of human malignancies, long-established human cell lines and many transgenic mouse models often fail to adequately predict drug effects in the clinic, which has caused over 90% of clinical trials of new oncology drugs to fail to meet their primary endpoints in Phase III.<sup>20–22</sup> Here, we established the largest bank of HCC PDX models with a high and stable tumor take rate (42.2%) that recapitulated the key clinical and molecular characteristics of primary tumors. We demonstrated the potential application of the model in the examination of population-based *in vivo* compound screens, which could aid in the identification of responsive subpopulations, and enable a more personalized approach to patient therapy. The responses to sorafenib in the PDX model correlated with the corresponding clinical response in the patients. Thus, the PDX model could be used to identify clinically relevant mechanisms of drug resistance. These PDX models are valuable surrogates for HCC patients and might play important roles in translational research.

Our data also indicated that the preferential expression of molecular markers for HCC, such as Ki67, caspase-3 and AFP, was retained in the xenograft tumors. Serum AFP, an important serum marker for HCC diagnosis and surveillance, exhibited similar levels in patients and relative PDX models, which indicated that serum AFP levels might be used as a biomarker to monitor treatment response. In addition to histological and proteomic stability, the gene expression and SNP profiles were consistent between the PDX models and the corresponding parental tumors, as seen for other cancers.<sup>23,24</sup> More importantly, remarkable stability at the histological, protein and genomic levels was acquired over sequential passages. Therefore, the PDX models may be more clinically relevant than traditional oncology models and may improve the accuracy of drug response prediction.

PDX models are being used increasingly for antitumor drug discovery and prediction. A number of novel drugs, such as the c-Met inhibitor LZ-8, the anti-CD47 monoclonal antibody B6H12 and the JAK1/2 inhibitor ruxolitinib, were recently tested in PDX clinical trials.<sup>25–27</sup> In our study, several antitumor agents were tested individually in a cohort including 16 selected PDX models, which resulted in a high degree of pharmacologic heterogeneity in the cohort. Disparate responses to different agents were also observed in the same model, and we found that treatment with the five agents resulted in different TGIs in the PDX model. Preliminary data showed that Sorafenib responses were consistent between patients and corresponding PDX models, suggesting the possibility that the model could accurately predict drug effects in the clinic. Hence, these results emphasize the importance of individualized treatments in clinical practice and the preclinical value of the PDX model in the treatment of HCC.

Recently, attention has been focused on the clinical application of PDX models on “precision medicine” by elucidating biomarkers that predict the sensitivity to an antitumor agent. In this case, PDX models that were characterized at the molecular level were an excellent *in vivo* system for exploring predictive biomarkers of various targeted agents. Sorafenib is currently the only systemic treatment for patients with advanced HCC approved by the US Food and Drug Administration. However, it has limited survival benefits and very poor tumor response.<sup>5</sup> Doctors need ideal biomarkers to predict sorafenib sensitization in clinical setting. Gene expression and SNP data in the sorafenib-sensitive and resistant PDX models indicated that MAP3K1 may be a predictor of sorafenib response in HCC. Based on the retrospective analysis of 78 HCC patients using sorafenib, we found that patients with high MAP3K1 expression exhibited superior postoperative survival after treatment with sorafenib. Prior reports showed that MAP3K1 regulates normal cellular proliferation, survival, differentiation, adhesion and motility by activation of the MAPK pathway.<sup>28</sup> The differential expression of MAP3K1 might activate/inactivate some signal transduction cascades, such as nerve growth factor signaling and stress-activated

protein kinases/JNK signaling. Although the mechanism of MAP3K1 in the response to sorafenib has not yet been elucidated, our data implied that MAP3K1 might be a potential biomarker for predicting sorafenib response; however, clinical investigations involving a large sample size are necessary to confirm this theory. Although we did not find any variants with genome-wide significance based on different sorafenib response, this might be owing to the small sample size of this study. Therefore, we did not exclude the possibility of finding sorafenib associated variants if large sample size is available.

Before implementing widespread use of PDX models, it is necessary to obtain higher and more stable tumor take rates and perform drug screening and toxicity studies. However, the factors leading to effective engraftment remain unclear. Engraftment failure remains high for HCC (approximately 20–35% tumor take rate).<sup>17,18</sup> Using tissue fragments coated in growth factors and Matrigel™ after implantation using a No. 20 trocar, the tumor take rates increased to 42.2%. A likely reason for the increased tumor take rate is that the addition of growth factors strongly promoted angiogenesis similar to previous studies in tumor cell lines.<sup>29,30</sup> Another possible explanation is that the rapid transfer of tumors without necrotic tissue and the use of a collagen matrix might help improve the survival of malignant cells that provide survival signals through integrin receptors and related proteins.<sup>31</sup> The use of trocar simplified the complex skin incision procedures, which reduced failure rates caused by infection. It is worth noting that Gu *et al.* did not use the same PDX passages as our current study so it could account for the potential difference between our studies and previous studies. For our future studies, a bioequivalence test will be performed to further strengthen our conclusion.

The enriched genes encoding for extracellular matrix were downregulated in xenografts compared to parental tumors similar to previous reports,<sup>32,33</sup> suggesting a loss of human tumor stroma. Histological analyses also confirmed that the human stroma was gradually replaced by host murine stroma after sequential passages. Although the drug response could be maintained in the PDX models from different passages,<sup>34,35</sup> the substitute of murine stroma after sequential passages would limit research of agents directed against the stromal compartment, such as blood vessels, fibroblasts and extracellular

matrix.<sup>36</sup> Thus, it is necessary to develop a reliable method for xenograft tumor tissue cryopreservation to minimize the effects of sequential passage. The take rate of the cryopreserved xenograft tissues was highest when FBS and 10% DMSO were used compared to other cryoprotectants. The xenografts retained their molecular stability before and after cryopreservation, which was confirmed by gene expression and SNP data.

A major problem of HCC treatments is the high incidence of recurrence (50–70% at 5 years).<sup>37</sup> Previous reports on the use of PDX models in HCC provided limited information regarding patient outcomes. We demonstrated that HCC patients whose tumors successfully engrafted had a higher recurrence rate (68.0% vs. 36.4%,  $p < 0.001$ ), indicating that tumor grafting is not only a promising tool for making HCC treatment decisions but also for identifying more aggressive, higher metastatic/recurrent tumors. Increased CSC biomarker expression, considered key factors for tumor relapse and drug resistance during treatment,<sup>38,39</sup> was also observed in stable tumor engraftments. Thus, these models provided a new method to further current understanding of the mechanisms of HCC metastasis and recurrence.

Here, we established a large collection of PDX models with a high and stable tumor take rate in HCC and a method for conservation. With further expansion of our xenograft bank, our PDX model could have a great impact in the preclinical drug discovery setting and in the identification of drug-resistant biomarkers, facilitating the development of individual therapies for HCC patients.

### Acknowledgements

This study was supported by grants from the National High Technology Research and Development Program (863 Program) of China (2015AA020401), the National Key Sci-Tech Project (2013ZX10002010-003, 2013ZX10002010-004, 2013ZX10002011-004 and 2012ZX0930100-007), the State Key Program of National Natural Science of China (81530077), the National Natural Science Foundation of China (81802364, 81772551, 81672839, 81472676, 81572064, 81572823, 81502028, 81572884 and 81372317), the Projects from the Shanghai Science and Technology Commission (13140901900, 14DZ1940300, 14411970200 and 14140902301), Specialized Research Fund for the Doctoral Program of Higher Education and Research Grants Council Earmarked Research Grants Joint Research Scheme (20130071140008), Shanghai Municipal Commission of Science and Technology (15YF1414100), and “Strategic Priority Research Program” of the Chinese Academy of Sciences (XDA12010201, 12020103 and 12020105).

### References

- Maluccio M, Covey A. Recent progress in understanding, diagnosing, and treating hepatocellular carcinoma. *CA Cancer J Clin* 2012;62:394–9.
- Jemal A, Bray F, Center MM, et al. Global cancer statistics. *CA Cancer J Clin* 2011;61:69–90.
- Forner A, Llovet JM, Bruix J. Hepatocellular carcinoma. *Lancet* 2012;379:1245–55.
- Peckradosavljevic M, Greten TF, Lammer J, et al. Consensus on the current use of sorafenib for the treatment of hepatocellular carcinoma. *Eur J Gastroenterol Hepatol* 2010;22:391–8.
- Gauthier A, Ho M. Role of sorafenib in the treatment of advanced hepatocellular carcinoma: an update. *Hepatol Res* 2013;43:147–54.
- Llovet JM, Borbath I, Ricci S, et al. Sorafenib in advanced hepatocellular carcinoma. *N Engl J Med* 2008;359:378–90.
- Gould SE, Juntila MR, de Sauvage FJ. Translational value of mouse models in oncology drug development. *Nat Med* 2015;21:431–9.
- Garber K. From human to mouse and Back: “Tumorgraft” models surge in popularity. *J Natl Cancer Inst* 2009;101:6–8.
- Daniel VC, Marchionni L, Hierman JS, et al. A primary xenograft model of small-cell lung cancer reveals irreversible changes in gene expression imposed by culture in vitro. *Cancer Res* 2009;69:3364–73.
- Gao H, Korn JM, Ferretti S, et al. High-throughput screening using patient-derived tumor xenografts to predict clinical trial drug response. *Nat Med* 2015;21:1318–25.
- Pavia-Jiménez A, Tcheuyap VT, Brugarolas J. Establishing a human renal cell carcinoma tumorgraft platform for preclinical drug testing. *Nat Protoc* 2014;9:1848–59.

12. Pena-Llopis S, Vega-Rubin-de-Celis S, Liao A, et al. BAP1 loss defines a new class of renal cell carcinoma. *Nat Genet* 2012;44:751–9.
13. Gu Q, Zhang B, Sun H, et al. Genomic characterization of a large panel of patient-derived hepatocellular carcinoma xenograft tumor models for preclinical development. *Oncotarget* 2015;6:20160–76.
14. Yang XR, Xu Y, Yu B, et al. High expression levels of putative hepatic stem/progenitor cell biomarkers related to tumour angiogenesis and poor prognosis of hepatocellular carcinoma. *Gut* 2010;59:953–62.
15. Qiu Z, Zou K, Zhuang L, et al. Hepatocellular carcinoma cell lines retain the genomic and transcriptomic landscapes of primary human cancers. *Sci Rep* 2016;6:27411.
16. Teicher BA, Andrews PA. *Anticancer drug development guide: preclinical screening, clinical trials, and approval*, vol. 1. New York, NY: Humana Press, 2004.
17. Yan M, Li H, Zhao F, et al. Establishment of NOD/SCID mouse models of human hepatocellular carcinoma via subcutaneous transplantation of histologically intact tumor tissue. *Chin J Cancer Res* 2013;25:289–98.
18. Xin H, Wang K, Hu G, et al. Establishment and characterization of 7 novel hepatocellular carcinoma cell lines from patient-derived tumor xenografts. *PLoS One* 2014;9:e85308.
19. Karandikar M, Xu S, Cobb MH. MEKK1 binds Raf-1 and the ERK2 Cascade components. *J Biol Chem* 2000;275:40120–7.
20. Choi SYC, Lin D, Gout PW, et al. Lessons from patient-derived xenografts for better in vitro modeling of human cancer. *Adv Drug Deliv Rev* 2014;79:222–37.
21. Roberts TG Jr, Goulart BH, Squitieri L, et al. Trends in the risks and benefits to patients with cancer participating in phase 1 clinical trials. *JAMA* 2004;292:2130–40.
22. Reichert JM, Wenger JB. Development trends for new cancer therapeutics and vaccines. *Drug Discov Today* 2008;13:30–7.
23. Zhang X, Claerhout S, Prat A, et al. A renewable tissue resource of phenotypically stable, biologically and ethnically diverse, patient-derived human breast cancer Xenograft models. *Cancer Res* 2013;73:4885–97.
24. Julien S, Merino-Trigo A, Lacroix L, et al. Characterization of a large panel of patient-derived tumor xenografts representing the clinical heterogeneity of human colorectal cancer. *Clin Cancer Res* 2012;18:5314–28.
25. Wu JR, Hu CT, You RI, et al. Preclinical trials for prevention of tumor progression of hepatocellular carcinoma by LZ-8 targeting c-met dependent and independent pathways. *PLoS One* 2015;10:e0114495.
26. Lo J, Lau EY, So FT, et al. Anti-CD47 antibody suppresses tumour growth and augments the effect of chemotherapy treatment in hepatocellular carcinoma. *Liver Int* 2016;36:737–45.
27. Yang S, Luo C, Gu Q, et al. Activating JAK1 mutation may predict the sensitivity of JAK–STAT inhibition in hepatocellular carcinoma. *Oncotarget* 2015;7:5461–9.
28. Kolch W, Kotwaliwale A, Vass K, et al. The role of Raf kinases in malignant transformation. *Expert Rev Mol Med* 2002;4:1–18.
29. Lee J, Kotliarova S, Kotliarov Y, et al. Tumor stem cells derived from glioblastomas cultured in bFGF and EGF more closely mirror the phenotype and genotype of primary tumors than do serum-cultured cell lines. *Cancer Cell* 2006;9:391–403.
30. Sakuma K, Aoki M, Kannagi R. Transcription factors c-Myc and CDX2 mediate E-selectin ligand expression in colon cancer cells undergoing EGF/bFGF-induced epithelial-mesenchymal transition. *Proc Natl Acad Sci U S A* 2012;109:7776–81.
31. Aparicio S, Hidalgo M, Kung AL. Examining the utility of patient-derived xenograft mouse models. *Nat Rev Cancer* 2015;15:311–6.
32. DeRose YS, Wang G, Lin YC, et al. Tumor grafts derived from women with breast cancer authentically reflect tumor pathology, growth, metastasis and disease outcomes. *Nat Med* 2011;17:1514–20.
33. Tentler JJ, Tan AC, Weekes CD, et al. Patient-derived tumour xenografts as models for oncology drug development. *Nat Rev Clin Oncol* 2012;9:338–50.
34. Keysar SB, Astling DP, Anderson RT, et al. A patient tumor transplant model of squamous cell cancer identifies PI3K inhibitors as candidate therapeutics in defined molecular bins. *Mol Oncol* 2013;7:776–90.
35. Rubio-Viqueira B, Jimeno A, Cusatis G, et al. An in vivo platform for translational drug development in pancreatic cancer. *Clin Cancer Res* 2006;12:4652–61.
36. Junttila MR, de Sauvage FJ. Influence of tumour micro-environment heterogeneity on therapeutic response. *Nature* 2013;501:346–54.
37. Cha C, Fong Y, Jarnagin WR, et al. Predictors and patterns of recurrence after resection of hepatocellular carcinoma. *J Am Coll Surg* 2003;197:753–8.
38. Maccalli C, De Maria R. Cancer stem cells: perspectives for therapeutic targeting. *Cancer Immunol Immunother* 2015;64:91–7.
39. Ajani JA, Song S, Hochster HS, et al. Cancer stem cells: the promise and the potential. *Semin Oncol* 2015;42(Suppl 1):S3–17.